FFEMS Fatigue & Fracture of Engineering Materials & Structures
ORIGINAL CONTRIBUTION
doi: 10.1111/ffe.12629

An approximation in closed form for the integral of Oore–Burns for cracks similar to a star domain

P. LIVIERI[1] and F. SEGALA[2]

[1]*Department of Engineering, University of Ferrara, via Saragat 1, 44122, Ferrara, Italy,* [2]*Department of Physics, University of Ferrara, via Saragat 1, 44122, Ferrara, Italy*

Received Date: 29 December 2016; Accepted Date: 13 April 2017; Published Online:

ABSTRACT In this paper, we give an explicit new formulation for the three-dimensional mode I weight function of Oore–Burns in the case where the crack border agrees with a star domain. Analysis in the complex field allows us to establish the asymptotic behaviour of the Riemann sums of the Oore–Burns integral in terms of the Fourier expansion of the crack border. The new approach gives remarkable accuracy in the computation of the Oore–Burns integral with the advantage of reducing the size of the mesh.
Furthermore, the asymptotic behaviour of the stress intensity factor at the tip of an elliptical crack subjected to uniform tensile stress is carefully evaluated. The obtained analytical equation shows that the error of the Oore–Burns integral tends to zero when the ratio between the ellipse axes tends to zero as further confirmation of its goodness of fit.

Keywords 3D weigh function; fracture mechanics; stress intensity factor.

NOMENCLATURE

a,b = dimensionless semi-axis of an elliptical crack
$\overline{a}, \overline{b}$ = actual semi-axis of an elliptical crack
e = eccentricity of ellipse
k_I = mode I stress intensity factor for a dimensionless domain
u, v = auxiliary dimensionless coordinate system
x, y = dimensionless Cartesian coordinate system
$\overline{x}, \overline{y}$ = actual Cartesian coordinate system
$E(e)$ = elliptical integral of second kind
K_{I2} = Taylor expansion up to second order of K_{I} for an ellipse
$K(e)$ = elliptical integral of first kind
K_I = mode I stress intensity factor
K_{Irw} = mode I stress intensity factor from Irwin's equation
Q = point of Ω
Q' = point of crack border
δ = size of mesh over crack
Δ = distance between Q and $\partial\Omega$
σ_n = nominal tensile stress in $\overline{x}, \overline{y}$ actual Cartesian coordinate system
σ = nominal tensile stress in $\overline{x}, \overline{y}$ dimensionless Cartesian coordinate system
Ω = crack shape
$\partial\Omega$ = crack border

INTRODUCTION

The advantages of the use of weight functions for the assessment of stress intensity factors (SIFs) are well known in the literature, especially when many loads act on the component. For each geometry, we have to estimate the correct weight function related to the location where the crack nucleates and then propagates under fatigue loading. For a correct evaluation of the SIF, the proper weight function should be calculated;

Correspondence: P. Livieri. E-mail: paolo.livieri@unife.it

however, accurate results can be obtained by generalising the weight function derived from the displacement function of Petroski and Achenbach.[1,2] On the basis of the procedure developed by Glinka and Shen,[1] by means of finite element analysis, we can obtain the parameter that appears as unknown in the generalised weight function proposed by Sha and Yang.[2] Applications to semi-elliptical cracks[3–5] or corner cracks[6] are present in the literature and show the efficiency in the evaluation of the SIF with error in the order of a few per cent with respect to the finite element results.

For a crack with an irregular shape, the calculation of the SIF is more complex and requires more effort. In fact, in order to evaluate the fatigue limit for materials with small notches or defects under mode I loading, Murakami and Endo[7] considered an average value of the SIF obtained from convex flaws. Murakami[8] suggested a shape factor, referred to as the square root of the area, about 0.5 for an engineering estimation of the maximum SIF for an arbitrarily 3D internal crack or 0.65 for an arbitrarily 3D surface crack.[9]

Some analytical weight functions available in the literature are able to relate the SIF at each point of an embedded planar two-dimensional crack subjected to mode I loading[10–14] or under mixed mode loading.[15,16] The Oore-Burns[12] weight function displays a simple analytic form and gives an exact result in the special cases of penny-shaped cracks or tunnel cracks. Furthermore, this weight function can be used for surface cracks after the introduction of proper coefficients inferred from classical analysis of a surface elliptical crack such as Normal-Rauj equations (see for instance refinements).[17,18] Obviously, the effect of vertex singularities is not taken into account because accurate studies are needed.[19,20] By means of the Oore–Burns weight, an engineering answer will be given without being too time consuming.[17,18] In this way, for example, the stress can be evaluated along the front crack for the estimation of the fatigue safety factor.[21–23]

Despite its very compact analytical expression, the numerical evaluation of the Oore–Burns integral (hereinafter, OB integral) is very difficult, due to the singular nature of the weight function, and special integration techniques are required as indicated by Desjardins *et al.*[24] and S. R. Montenegro *et al.*[25]

For the special case of ellipse cracks, the authors obtained a careful closed-form representation of the OB integral along elliptic cracks under general pressure from previous papers. More precisely, they found a closed expression of the second-order Taylor expansion of the SIFs with respect to deviation of the ellipse from the disc for a generic tensile stress over the crack.[26] The

Table 1 Comparison between the prediction in stress intensity factor (SIF) from Eq. (17) and Irwin exact solution as a function of mesh refinements for a circular crack (σ_n and σ are the uniform tensile stresses, $\bar{a}$ is the radius of the crack, and $M\delta = \pi$)

M	δ	Irwin[28] $\frac{K_{Irw}}{\sigma_n\sqrt{\bar{a}}}$	$\frac{K_I}{\sigma_n\sqrt{\bar{a}}}$ from Eq. (17) without the correction term $0.927\,\sigma\left(Q'\right)\sqrt{\delta}$	$e_{\%}$ per cent error compared with Irwin[28] solution [%]	$\frac{k_I}{\sigma}$ from Eq. (17)	$e_{\%}$ per cent error compared with Irwin[28] solution [%]	Numerical extrapolation C
25	0.125664	1.12838	0.80461	28.7	1.13322	−0.43	–
50	0.062832	1.12838	0.89781	20.4	1.13018	−0.16	0.898
100	0.031416	1.12838	0.96477	14.5	1.12908	−0.06	0.912
200	0.015708	1.12838	1.01246	10.3	1.12864	−0.02	0.919
400	0.007854	1.12838	1.04632	7.3	1.12847	−0.01	0.922
800	0.003927	1.12838	1.07031	5.1	1.12840	0.00	0.925
1600	0.001963	1.12838	1.08730	3.6	1.12838	0.00	0.926
3200	0.000982	1.12838	1.09933	2.6	1.12837	0.00	0.926
6400	0.000491	1.12838	1.10783	1.8	1.12837	0.00	0.927

deviation of an ellipse from the disc is quantitatively described by the parameter $\varepsilon = 1 - b/a$, where a and b are the major and minor semi-axes respectively. The exact evaluation of the OB integral by means of an explicit quadrature formula with a polar integration grid was also considered by the authors in Ref. 27. Our approach drastically reduces the computational time to evaluate the OB integral because a very coarse mesh is sufficient without loss of accuracy. This was made possible by theoretical evaluation of the coefficient of $\delta^{1/2}$ in the deviation between the integral and its Riemann sum (δ is the size of the mesh over the crack).

We will show that the convergence is extremely fast (Tables 2 & 3). The aim of this paper is to permanently optimize the previous algorithm and to extend it to a general equation for irregular inner cracks like to a star domain (and hence every convex crack). The equation is derived from the Oore–Burns weight function by means of complex analysis. The coefficient of $\delta^{1/2}$ in the expansion of the Riemann sum of Oore–Burns was evaluated with an accuracy never previously achieved, and this is new with respect to our previous papers, in particular Ref. 27. Furthermore, in the case of elliptical cracks under uniform tensile loading, the gap between

Table 2 Comparison with Irwin exact solution as a function of mesh refinements for an ellipse (σ_n and σ are the uniform tensile stresses, $\bar{b}$ is the minor semi-axis of the ellipse, $\bar{a}$ is the maximum semi-axis of the ellipse, and $M\delta = \pi$)

M	$\bar{b}/\bar{a}$	θ [deg]	δ	Irwin[28] $\frac{K_{Irw}}{\sigma_n\sqrt{\bar{a}}}$	From Eq. (29) $\frac{k_I}{\sigma}$	$e_{\%}$ per cent error compared with Irwin[28] solution [%]
100	0.8	0°	0.031416	0.999915	1.01379	1.39
200	0.8	0°	0.015708	0.999915	1.01312	1.32
400	0.8	0°	0.007854	0.999915	1.01280	1.29
800	0.8	0°	0.003927	0.999915	1.01268	1.28
1600	0.8	0°	0.001963	0.999915	1.01264	1.27
100	0.8	45°	0.031416	1.063829	1.06374	0.01
200	0.8	45°	0.015708	1.063829	1.06326	0.05
400	0.8	45°	0.007854	1.063829	1.06305	0.07
800	0.8	45°	0.003927	1.063829	1.06296	0.08
1600	0.8	45°	0.001963	1.063829	1.06293	0.08
100	0.8	90°	0.031416	1.117939	1.10756	0.93
200	0.8	90°	0.015708	1.117939	1.10715	0.97
400	0.8	90°	0.007854	1.117939	1.10697	0.98
800	0.8	90°	0.003927	1.117939	1.10690	0.99
1600	0.8	90°	0.001963	1.117939	1.10688	0.99

Table 3 Comparison with Irwin exact solution as a function of mesh refinements for an ellipse (σ_n and σ are the uniform tensile stresses, $\bar{b}$ is the minor semi-axis of the ellipse, $\bar{a}$ is the maximum semi-axis of the ellipse, and $M\delta = \pi$)

M	$\bar{b}/\bar{a}$	θ [deg]	δ	Irwin[28] $\frac{K_{Irw}}{\sigma_n\sqrt{\bar{a}}}$	From Eq. (29) $\frac{k_I}{\sigma}$	$e_{\%}$ per cent error compared with Irwin[28] solution [%]
100	0.6	0°	0.031416	0.833214	0.86411	3.71
200	0.6	0°	0.015708	0.833214	0.86290	3.56
400	0.6	0°	0.007854	0.833214	0.86234	3.50
800	0.6	0°	0.003927	0.833214	0.86215	3.47
1600	0.6	0°	0.001963	0.833214	0.86207	3.46
100	0.6	45°	0.031416	0.976805	0.97406	0.28
200	0.6	45°	0.015708	0.976805	0.97343	0.35
400	0.6	45°	0.007854	0.976805	0.97322	0.37
800	0.6	45°	0.003927	0.976805	0.97313	0.38
1600	0.6	45°	0.001963	0.976805	0.97310	0.38
100	0.6	90°	0.031416	1.075674	1.05510	1.91
200	0.6	90°	0.015708	1.075674	1.05474	1.95
400	0.6	90°	0.007854	1.075674	1.05458	1.96
800	0.6	90°	0.003927	1.075674	1.05454	1.97
1600	0.6	90°	0.001963	1.075674	1.05452	1.97

the OB integral and the Irwin analytic solution is discussed. Finally, a comparison of the SIFs between the proposed equations and those taken from the literature will show the validity of the solution.

BACKGROUND

The SIFs of the mode I loading of a planar crack Ω in a three-dimensional body can be made by means of the Oore–Burns[12] relationship that agrees with the known results when the crack takes a special configuration such as a disc or a tunnel crack.

Let Ω be an open bounded simply connected subset of the plane and

$$f(Q) = \int_{\partial\Omega} \frac{ds}{|Q - P(s)|^2}\ ,\ Q \in \Omega \tag{1}$$

where s is the arch-length on $\partial\Omega$ and $P(s)$ describes $\partial\Omega$. Oore and Burns proposed the following expression for the mode I SIF at every point $Q' \in \partial\Omega$ when the crack is subjected to a nominal tensile loading $s_n(Q)$:

$$K_I\left(Q'\right) = \frac{\sqrt{2}}{\pi} \int_{\Omega} \frac{\sigma_n(Q)\, h(Q)}{\left|Q - Q'\right|^2} d\Omega\ , \qquad Q' \in \partial\Omega \tag{2}$$

where

$$h(Q) = \frac{1}{\sqrt{f(Q)}} \tag{3}$$

Under reasonable conditions on the nominal stress σ_n (Q), the integral (2) is convergent (see for instance Ref. 29).

APPROXIMATION FORMULA

From now on, we will assume that the boundary of the crack is locally a graph of a C^1 function. In order to simplify the analytical formulation of K_I, it is convenient to consider a dimensionless domain obtained by means of a linear isotropic dilatation. The actual crack will be distinguished by means of an upper line bar, so that $\overline{\Omega}$ is the initial crack and Ω is the dimensionless reference domain. We take Ω as a reference domain in such a way that the maximum diameter of Ω is equal to 2. We are able to reconstruct the SIF K_I for the actual domain $\overline{\Omega}$ (which is a dilation of a domain Ω) from the identity $\overline{\Omega} = \lambda\Omega$. The relation between K_I and the SIF evaluated for a dimensionless domain k_I is given by

$$K_I\left(\overline{Q}', \sigma_n(\overline{Q})\right) = \sqrt{\lambda}\, k_I\left(Q', \sigma_n(\lambda Q)\right) \tag{4}$$

where the meaning of the notation is clear and σ_n is the nominal tensile stress evaluated without the presence of the crack being the actual domain $\overline{\Omega}$ (Fig. 1). Note that λ is a scalar quantity that has a physical dimension equal to a length, whereas the physical dimension of k_1 is a pressure.

We fix an orthogonal Cartesian reference x,y of which the origin is, for example, the centre of mass of Ω. Every point Q' on $\partial\Omega$ will be identified by its distance in terms of arc length from a fixed point Q'_0 on the boundary. We introduce a new orthogonal Cartesian reference (u,v) centred in Q' by following Fig. 2. A point Q can be represented in the forms $x \cdot e_1 + y \cdot e_2$ and $u \cdot k_1 + v \cdot k_2$, where e_1, e_2, k_1 and k_2 are the versors of the axes x,y,u,v. We considered the polar mesh given by the points

$$Q_{j,k} = k\delta\left(k_1 \cos j\delta + k_2 \cos j\delta\right) \tag{5}$$

with δ the small submultiple of $\pi/2$ and

$$k \geq 0, \qquad 0 \leq j \leq 2M - 1, \qquad M\delta = \pi \tag{6}$$

On the boundary $\partial\Omega$, we introduce a discretisation of size $\tau = L/[L/\delta]$, where L is the length of $\partial\Omega$ and [] means the integer part. We denote by P_{mjk} the point of $\partial\Omega$ of which the distance (in terms of arc length) from the

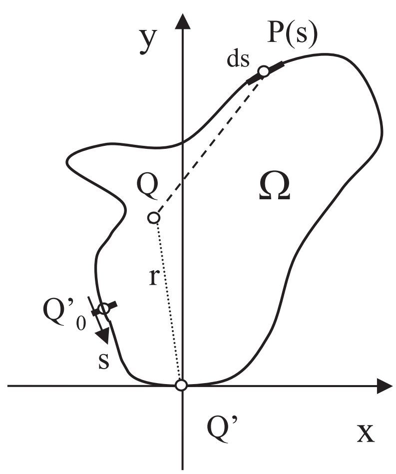

Fig. 1 Planar irregular crack.

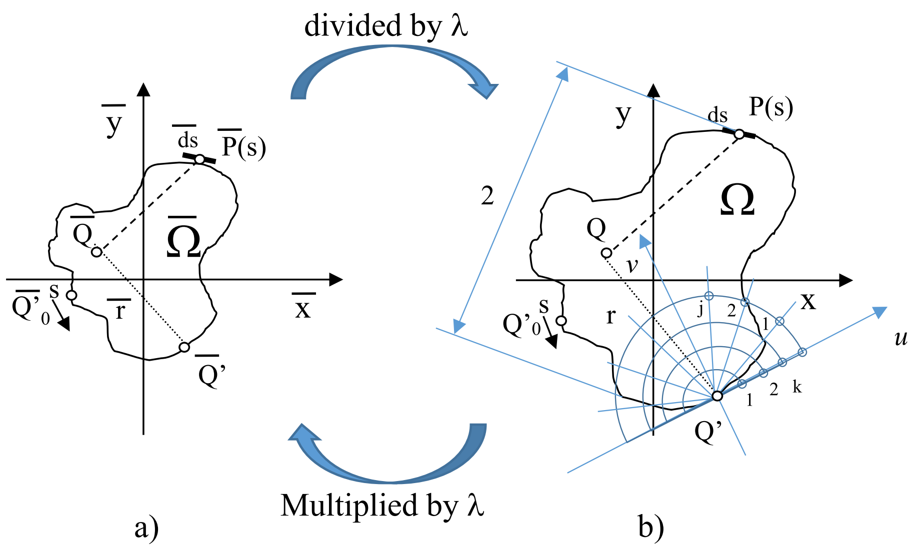

Fig. 2 (a) Actual crack and (b) dimensionless crack integration domain with semi diameter equal to unity with the mesh for numerical computation. [Colour figure can be viewed at wileyonlinelibrary.com]

projection of Q_{jk} on $\partial\Omega$ is $m \cdot \tau$. Obviously, m runs on the range

$$0 \le m \le \left[\frac{L}{\pi} M\right] - 1 \tag{7}$$

By refining the techniques developed in previous work,[27] we are able to establish an ultimate convergence formula for the integral (2). In order to lighten the notation, we put

$$A_{jk} = \left(\sum \left|Q_{jk} - P_{mjk}\right|^{-2}\right)^{-1/2} \tag{8}$$

where the sum is on the index m in its natural range (7),

$$I = \int_0^{\pi} \sqrt{\sin\vartheta}\, d\vartheta \tag{9}$$

$$\mathcal{J} = \int_0^1 \sqrt{\vartheta\, th(\pi\vartheta)}\, d\vartheta \tag{10}$$

$$F = \int_0^1 \frac{\sqrt{\vartheta}\left(1 - \sqrt{th(\pi\vartheta)}\right)}{\sqrt{1-\vartheta^2}}\, d\vartheta \tag{11}$$

$$H = \int_0^{\infty} \sqrt{\vartheta}\, e^{-2\pi\vartheta}\, d\vartheta \tag{12}$$

$$C = -\frac{\sqrt{2}}{\pi^{3/2}} I\zeta(1/2) + \frac{2\sqrt{2}}{\pi^{3/2}}\left[F + \left(\frac{\pi^2}{6} - 1\right)\left(\frac{2}{3} - \mathcal{J}\right)\right] + \frac{\sqrt{2}\pi}{3} H \tag{13}$$

In Eq. (13), ζ represents the zeta Riemann function. Then, the approximation formula is the following:

$$k_I\left(Q'\right) = \left[\frac{\sqrt{2}}{\pi} \sum_{jk} \frac{A_{jk}}{k}\, \sigma\left(Q_{jk}\right) + C\,\sigma\left(Q'\right)\right]\sqrt{\delta} + O(\delta) \tag{14}$$

The sum on the right-hand side (r.h.s.) of Eq. (14) is on the indexes jk for which $Q_{ik} \in \Omega$. By inserting a numerical value, we obtain

$$C = 0.932854\ldots \tag{15}$$

(see Ref. [27]). The proof of Eq. (14) is based on some proprieties of the ζ function, Riemann sums, the Stone-Weierstrass theorem and the identity

$$\sum_{-\infty}^{+\infty} \frac{1}{a^2 + n^2} = \frac{\pi}{a}\, \frac{1}{th(\pi a)}, \quad a \neq 0 \tag{16}$$

In order to greatly save computation time, in our simulations, we choose the discretisation on the boundary of Ω in such a way that the starting point is Q' (i.e. fixed) and P_m is the point with the coordinate of $m\tau$. This choice implies a slight correction of the coefficient

C in Eq. (13). The very delicate analysis is performed in the Appendix, of which we show that the correction is about $-5.35 \cdot 10^{-3}$. More precisely, Eq. (14) becomes

$$k_I\left(Q'\right)\approx\left[\frac{\sqrt{2}}{\pi}\sum_{jk}\frac{A_{jk}}{k}\,\sigma\left(Q_{jk}\right)+0.927\,\sigma\left(Q'\right)\right]\sqrt{\delta} \tag{17}$$

Remark 1

In terms of dimensional consistency, by calling δ_r, δ_θ and δ_s the size of the partitions on $R^2 \times \partial\Omega$, Eq. (17) is written as follows:

$$k_I\left(Q'\right)\approx\frac{\sqrt{2}}{\pi}\frac{\delta_\vartheta}{\sqrt{\delta_s}}\sum\frac{A_{jk}}{k}\,\sigma\left(Q_{jk}\right)+\left(0.889\sqrt{\delta_r}+0.038\frac{\delta_s^{3/2}}{\delta_r}\right)\sigma\left(Q'\right) \tag{18}$$

TEST ON THE UNITARY DISC

We test Eq. (17) on the unit disc of Fig. 3, in the case of uniform tensile stress σ. The fixed starting point on $\partial\Omega$ is $P_o = e_1$, that is, $P_m = \cos(m\delta)\cdot e_1 + \sin(m\delta)\cdot e_2$. The condition $Q_{jk}\in\Omega$ becomes

$$1\leq j\leq M-1,\qquad 1\leq k<\frac{2}{\delta}\sin(j\delta) \tag{19}$$

and from Eq. (7)

$$0\leq m\leq 2M-1 \tag{20}$$

Table 1 shows the accuracy of Eq. (17) in the prediction of the SIF. The theoretical value is equal to 1.275, as evaluated by Irwin[28] under uniform nominal stress σ. The theoretical expectation is completely satisfied also with a rough mesh. The value of C reported in Table 1 is the value obtained by means of the Richardson extrapolation from the result of the only Riemann sum. When the mesh is very accurate (M = 6400), the numerical prediction of C agrees with the theoretical one reported in Eq. (17). This is confirmation that this work permanently improves every other study on the subject.

UNITARY ELLIPTICAL CRACKS

In this section, we assume that Ω is a dimensionless ellipse contour $\frac{x^2}{a^2}+\frac{y^2}{b^2}\leq 1$ with $0<b\leq a=1$. The natural description of $\partial\Omega$ is given in terms of the angle θ related to Cartesian coordinates x,y by $x = a\cdot\cos\theta$, $y = b\sin\theta$ (Fig. 4). By Q', we mean the point $(a\cdot\cos\alpha)\,e_1 + (b\cdot\sin\alpha)\,e_2$. In this case, the link between x,y and u,v is given by

$$u=\frac{1}{g}\left(-a\sin\alpha x+b\cos\alpha y+\frac{a^2e^2}{2}\sin 2\alpha\right) \tag{21}$$

$$v=\frac{1}{g}\left(-b\cos\alpha x-a\sin\alpha y+ab\right) \tag{22}$$

$$x=\frac{1}{g}\left(-a\sin\alpha u-b\cos\alpha v+ag\cos 2\alpha\right) \tag{23}$$

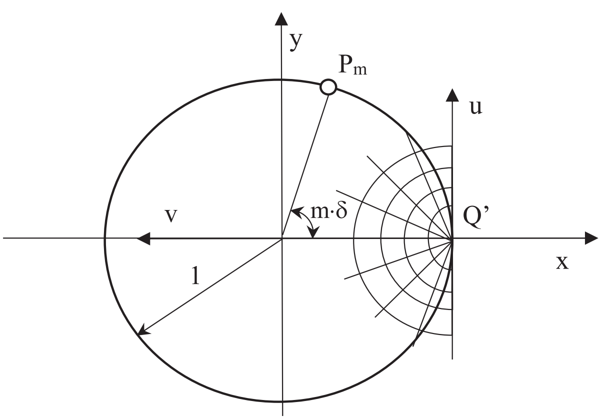

Fig. 3 Reference coordinate system for the calculation of k_I in point Q' in the case of a dimensionless unit circular crack.

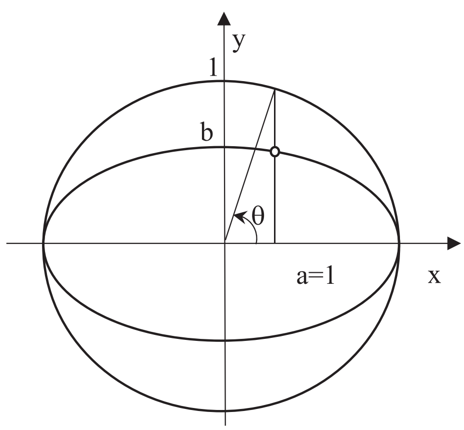

Fig. 4 Reference coordinate system for the calculation case of a dimensionless unit elliptical crack.

$$y = \frac{1}{g}\left(b\cos\alpha u - a\sin\alpha v + bg\sin\alpha\right) \tag{24}$$

where $e = \sqrt{1 - \frac{b^2}{a^2}}$ is the eccentricity of the ellipse and

$$g = g(\alpha) = a\sqrt{1 - e^2\cos^2\alpha} \tag{25}$$

Fixed e is denoted by $E(\phi)$, which is the complete elliptic integral of the second kind. Moreover, let

$$\vartheta_m = E^{-1}\left(m\delta + E\left(\frac{\pi}{2}\right)\right) - \frac{\pi}{2} \tag{26}$$

$$P_m = a\cos(\alpha + \vartheta_m)\,e_1 + b\sin(\alpha + \vartheta_m)\,e_2 \tag{27}$$

$$C_{jk} = \left(\sum_0^{2N-1}\left|Q_{jk} - P_m\right|^{-2}\right)^{-1/2} \tag{28}$$

By applying Eq. (17), it follows

$$k_I \approx \left[\frac{\sqrt{2}}{\pi}\sum\frac{C_{jk}}{k}\,\sigma\left(Q_{jk}\right) + 0.927\,\sigma\left(Q'\right)\right]\sqrt{\delta} \tag{29}$$

$$E = 0.889 + 0.038\left(1 - e^2\cos^2\alpha\right)^{3/4}\cos\left(\frac{2\pi}{\sqrt{1 - e^2\cos^2\alpha}}\right) \tag{32}$$

Equation (29) is amended as follows:

$$k_I = \left[\frac{\sqrt{2}}{\pi}\sum\frac{C^*_{jk}}{k}\,\sigma\left(Q_{jk}\right) + E\left(1 - e^2\,G\cos^2\alpha\right)\sigma\left(Q'\right)\right]\sqrt{\delta} + O(\delta) \tag{33}$$

where $G = G(\alpha, e)$ is a bounded function and $0 \le e^2 G \le 0.02$. By reading Q_{ik} and P_m in the reference (u,v), we have Q_{jk}, given by Eq. (5) and

$$P_m = \frac{a}{\sqrt{1 - e^2\cos^2(\alpha)}}\left[\sin(m\delta) - e^2\cos\alpha\left(\sin(\alpha + m\delta) - \sin(\alpha)\right)\right]k_1 + \frac{b}{\sqrt{1 - e^2\cos^2(\alpha)}}\left[1 - \cos(m\delta)\right]k_2 \tag{34}$$

We clarify the condition $Q_{jk} \in \Omega$ in the sum on the r.h.s. of Eq. (33). By Eqs (23) and (24), the request is equivalent to

$$1 \le j \le M - 1 \tag{35}$$

$$1 \le k < \frac{4}{\delta}\,\frac{\left(a^2\sin^2\alpha + b^2\cos^2\alpha\right)^{3/2} ab\sin(j\delta)}{2a^2b^2\cos^2(j\delta) + 2\left(a^4\sin^2\alpha + b^4\cos(\alpha)\right)\sin^2(j\delta) - ab\left(a^2 - b^2\right)\sin(2\alpha)\sin(2j\delta)} \tag{36}$$

Tables 2 and 3 show that the approximation (29) is absolutely confirmed. Obviously, when the b/a decreases, the per cent error increases due to the nature of the OB integral.[12,24,30]

We may speed up Eq. (29) (at least by a factor of 10) by choosing the mesh on $\partial\Omega$ in terms of the angle ϑ, rather than length s. The reason is to avoid the amplitude function E^{-1} which slows down the program heavily. Therefore, let

$$P_m = a\cos(\alpha + m\delta)\,e_1 + b\sin(\alpha + m\delta)\,e_2 \tag{30}$$

$$C^*_{jk} = \left(\sum_0^{2M-1}\left|Q_{jk} - P_m\right|^{-2}\sqrt{1 - e^2\cos^2(\alpha + m\delta)}\right)^{-1/2} \tag{31}$$

We may speed up Eqs (29) and (33) by a standard extrapolation argument. The conclusion is

$$k_I\left(Q'\right) = 2S\left(\frac{\delta}{2}\right) - S(\delta) + \left(\sqrt{2} - 1\right)E\sigma\left(Q'\right)\sqrt{\delta} + O\left(\delta^{3/2}\right) \tag{37}$$

where $S(\delta)$ represents the Riemann sum

$$S(\delta) = \frac{\sqrt{2\delta}}{\pi}\sum\frac{C_{jk}}{k}\,\sigma\left(Q_{jk}\right) \tag{38}$$

Table 4 reports a comparison with Irwin's exact solution and Eq. (33) as function of the a/b ratio. The

Table 4 Comparison with Irwin exact solution as a function of mesh refinements for an ellipse (σ$_n$ and σ are the uniform tensile stresses, $\bar{b}$ is the minor semi-axis of the ellipse, and $\bar{a}$ is the maximum semi-axis of the ellipse)

		Irwin[28]		From Ref.[26]
$\bar{b}/\bar{a}$	θ [deg]	$\frac{K_{Irw}}{\sigma_n\sqrt{\bar{a}}}$	From Eq. (33) (M = 800) $\frac{k_I}{\sigma}$	$\frac{K_{I2}}{\sigma_n\sqrt{\bar{a}}}$
0.9	0°	1.068	1.076	1.074
0.8	0°	1.000	1.014	1.014
0.7	0°	0.922	0.943	0.947
0.6	0°	0.833	0.863	0.874
0.5	0°	0.732	0.770	0.794
0.9	45°	1.098	1.099	1.099
0.8	45°	1.064	1.064	1.064
0.7	45°	1.024	1.023	1.026
0.6	45°	0.977	0.974	0.984
0.5	45°	0.920	0.915	0.938
0.9	90°	1.126	1.120	1.121
0.8	90°	1.118	1.107	1.109
0.7	90°	1.102	1.086	1.093
0.6	90°	1.076	1.055	1.073
0.5	90°	1.035	1.010	1.048

difference between the results obtained in Tables 3 and 4 is very small. Furthermore, the same table reports the calculation of the approximation K_{I2} of K_I obtained by means of a second-order approximation of the OB integral proposed in explicit form in Ref. [26]. The conclusion is that Eq. (29) has an essentially theoretical value. The equations that are really useful from an operational point of view are Eqs (33) and (37).

Now, we conclude this section with the analysis of the accuracy in the OB integral prediction in the classic case of an elliptical crack under uniform tensile loading.

As is well known, when b tends toward zero, the SIF at the notch tip radius tends to have a gap between the classical Irwin solution. In fact, for b/a equal to 0.2, Oore and Burns obtained a per cent error around 17%, whereas Desjardins *et al.*,[24] by means of an optimized numerical solution, calculated a value of 18.4%. Equation (33) gives a value of 17.5% with M = 3200. Montenegro *et al.*,[25] under the hypothesis that the error depends on the ellipse aspect ratio and on the local crack front curvature, introduced the corrective function f_c for the OB integral. On the other hand, in a previous paper,[30] the authors showed that, when an elliptical crack is assumed under uniform tensile loading, the OB integral gives a first-order approximation of SIF along the whole crack front, very close to the first order approximation of K_{Irw}, Irwin's exact solution. In particular, when the eccentricity e of the ellipse tends to zero, the principal contribution $\frac{e^2}{20\sqrt{\pi}}$ to the discrepancy is very small. However, Irwin's theoretical equation at the notch tip gives a value of the SIF that tends to zero when $b/a \to 0$. So that a more realistic comparison between the OB integral and the Irwin equation should be made on the basis of a weighted error of the type: $(K_I - K_{Irw})/K_{Irw,\max}$, where $K_{Irw,\max}$ is the maximum value of SIF for the crack with ratio b/a.

In order to evaluate the weighted error, we conclude this section by examining the asymptotic behaviour of the OB integral when $b/a \to 0$. For simplicity, it was assumed that a = 1. For uniform pressure σ = 1, the well-known result of Irwin is given by

$$I(\alpha) = \frac{\sqrt{\pi b}}{E(e)} \left(\sin^2\alpha + b^2\cos^2\alpha\right)^{1/4} \tag{39}$$

Therefore, for fixed $\alpha \in]0,\pi/2[$, one has

$$I(\alpha) \approx \sqrt{\pi \sin \alpha\, b},\ b \to 0 \tag{40}$$

and

$$I(0) \approx \sqrt{\pi\, b},\ b \to 0 \tag{41}$$

In view to find the behaviour of the OB integral for $b \to 0$, we need a preliminary estimate. By referring to Fig. 5, we put

$$\Delta = \text{distance}\,(Q, \partial\Omega) \tag{42}$$

$$Q^* = \text{projection of } Q \text{ on } \partial\,\Omega \tag{43}$$

Then, by Carnot

$$|Q - P(s)|^2 = \Delta^2 + |Q^* - P(s)|^2 - 2\,\Delta\,|Q^* - P(s)|\,\cos(\omega) \tag{44}$$

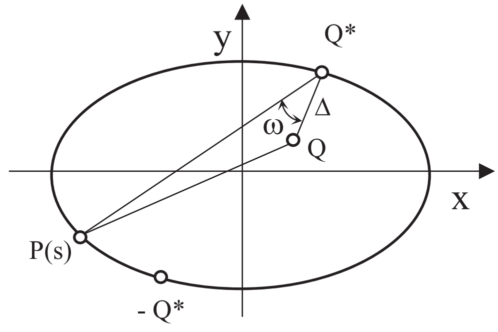

Fig. 5 Application to the Carnot theorem.

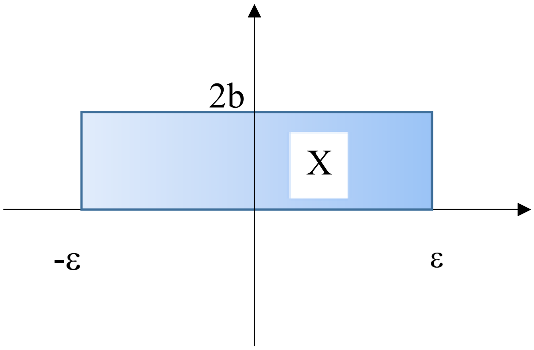

Fig. 6 Model of domain integration for the asymptotic behaviour of Oore–Burns integral. [Colour figure can be viewed at wileyonlinelibrary.com]

On convex sets, $\omega < \pi/2$. We consider Q^* the origin on $\partial\Omega$, and so in terms of arc length, the coordinate of $-Q^*$ is $-L \equiv L$, $2L$ being the length of the ellipse. By taking into account $|Q^* - P(s)| \leq s$, from Eq. (44), it follows that

$$|Q - P(s)|^2 = \Delta^2 + s^2 \tag{45}$$

and then

$$f(Q) \geq \frac{\pi}{\Delta}\left(1 - \frac{b}{\pi}\right) \tag{46}$$

$$h(Q) \leq \frac{\sqrt{\Delta}}{\sqrt{\pi}}(1 + O(b)) \approx \frac{\sqrt{\Delta}}{\sqrt{\pi}}, b \to 0 \tag{47}$$

When $\alpha \neq 0$, we consider, for example, $\alpha = \pi/2$. Then, by Fig. 6, the asymptotic behaviour of Oore–Burns is given by the model

$$k_I = \frac{\sqrt{2}}{\pi}\frac{1}{\sqrt{\pi}}\frac{1}{\sqrt{2b}}\int_X \frac{\sqrt{y}\sqrt{2b - y}}{x^2 + y^2}\,dx\,dy = \sqrt{\pi b} + O\left(b^{3/2}\right) \tag{48}$$

In a similar way, it is not difficult to verify that for $\alpha \neq 0$, the asymptotic behaviour of Irwin and Oore-Burns agrees. The problem is for $\alpha = 0$. By putting $c = \frac{1}{2b^2}$, the model for Oore–Burns is given by

$$k_I = \frac{\sqrt{2}}{\pi}\int_Y \frac{b}{x^2 + y^2}\,dx\,dy \tag{49}$$

where Y is the set in Fig. 7a.

We divide region Y in four parts, by Fig. 7b. On regions Y_1 and Y_2, we make use of the estimate

$$\Delta \leq x - cy^2 \tag{50}$$

while on regions Y_3 and Y_4, we make use of the estimate

$$\Delta \leq \frac{1}{\sqrt{c}}\left(\sqrt{x} - \sqrt{c}\,|y|\right) \tag{51}$$

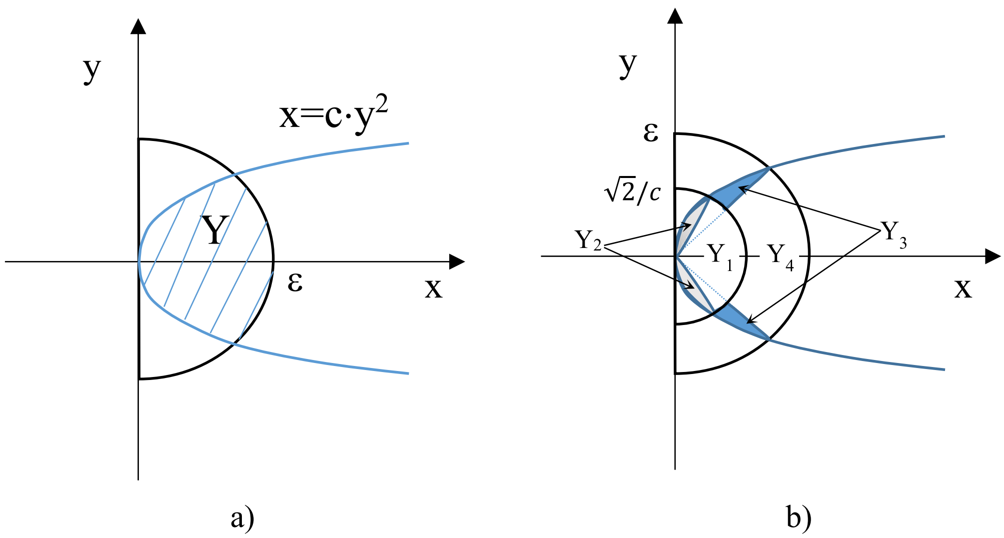

Fig. 7 (a) Domain integration for the asymptotic behaviour of Oore–Burns integral; (b) partition of the domain integration for the asymptotic behaviour of Oore–Burns integral. [Colour figure can be viewed at wileyonlinelibrary.com]

We illustrate, for example, the contribution coming from region Y_2. By Eqs (47), (49) and (50), we have to bind the integral

$$k_{Y2} = \frac{2\sqrt{2}}{\pi^{3/2}} \int_{R2} \frac{\sqrt{x - cy^2}}{x^2 + y^2}\, dx\, dy \tag{52}$$

By changing coordinates $x = \frac{z}{c \tan^2 \vartheta}$, $y = \frac{z}{c \tan \vartheta}$, we may compute k_{Y2}. Precisely

$$k_{Y2} = \frac{b \ln 2}{\sqrt{\pi}} \tag{53}$$

By taking the overall contributions into account, the OB integral for small b is bound by

$$k_I \le \frac{b}{\sqrt{\pi}} \left\{ \ln 2 + \int_0^{\pi/4} \left[\begin{array}{l} \frac{4 2^{1/4}}{\pi} \sqrt{\cos\vartheta - \sqrt{2}\sin^2\vartheta} + \frac{4}{\pi}\frac{1}{\tan\vartheta} \arcsin\left(2^{1/4}\sqrt{\cos\vartheta}\tan\vartheta\right) + \\ -\frac{8 2^{1/8}}{\pi}\sqrt{\sqrt{\cos\vartheta} - 2^{1/4}\sin\vartheta} - \frac{8}{\pi\sqrt{\tan\vartheta}} \arcsin\left(2^{1/8}\cos^{1/4}\vartheta\sqrt{\tan\vartheta} + \frac{4}{\sqrt{\tan\vartheta}}\right) \end{array} \right] d\vartheta \right\} \approx \approx 3.320\, b \tag{54}$$

A much more refined analysis of the function Δ allows us to improve the estimation (54) up to

$$k_I \le 2.90\, b \tag{55}$$

In virtue of Eq. (55), the weighted percentage of the error of Oore–Burns with respect to Irwin K_{Irw} (much more significant than a simple percentage) is then bound by

$$\frac{K_I - K_{Irw}}{K_{Irw,\max}} \le 0.63\sqrt{b}, b \to 0 \tag{56}$$

That is the weighed percentage →0 for $b \to 0$. The estimate (56) is presumably optimal and shows an excellent agreement with numerical simulations as reported in Fig. 8. When $b \sim 1$, the weighted percentage error $\sim \frac{\varepsilon}{20}\left(1 + \frac{9}{16}\varepsilon\right)$ with $\varepsilon = 1 - b$ (see Ref. [30]).

Finally, in this section, we make the comparison between Eq. (33) and the results of Irwin's equation. By calling I_2, the Taylor expansion of the second order of the Irwin SIF K_{Irw}, and K_{I2}, the Taylor expansion of the second order of the OB integral K_I, from Ref. [26] we obtain the approximation $K_I \approx K_{Irw} + K_{I2} - I_2$ precisely

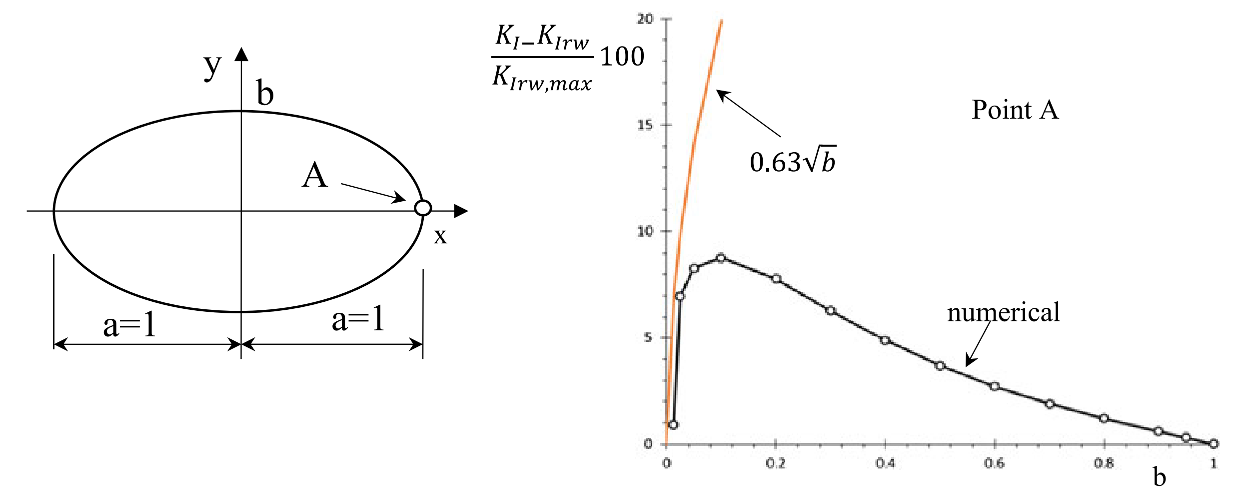

Fig. 8 Weighed percentage error at the tip in the case of a dimensionless elliptical crack as a function of the semi-axis b. [Colour figure can be viewed at wileyonlinelibrary.com]

up to 10^{-3} in the range of $0.5 \leq b \leq 1$. In Table 4, the agreement among the results obtained with different equation is satisfactory.

STAR DOMAINS

In this section, we assume that Ω will be a star domain. Therefore, we can read its boundary in terms of polar coordinates; that is, we assume that the boundary is discussed by a C^1 function $R = R(\vartheta), \vartheta \in [0, 2\pi]$. Of course, in this case, it is very useful to discretise $\partial\Omega$ in terms of the angle ϑ in order to speed up the numerical procedure. We take Ω dimensionless, by normalisation in such a way that $\max_{[0,2\pi]} \gamma = 1$, where

$$\gamma(\vartheta) = \sqrt{R^2(\vartheta) + R'^2(\vartheta)} \tag{57}$$

A careful analysis of our technique allows us to amend Eq. (14). Let α be the coordinate of the pole Q'.

$$P_m = R(\alpha + m\delta)\left(\cos(\alpha + m\delta)\, e_1 + \sin(\alpha + m\delta)\, e_2\right) \tag{58}$$

$$B_{jk} = \left(\sum_0^{2N-1} \left|Q_{jk} - P_m\right|^{-2} \gamma(\alpha + m\delta)\right)^{-1/2} \tag{59}$$

Hence, the approximation becomes

$$k_I\left(Q'\right) \approx \left[\frac{\sqrt{2}}{\pi} \sum_{jk} \frac{B_{jk}}{k}\, \sigma\left(Q_{jk}\right) + D\, \sigma\left(Q'\right)\right] \sqrt{\delta} \tag{60}$$

and the coefficient D is given by

$$D = 0.889 + 0.038\, \gamma(\alpha)^{\frac{3}{2}} \cos\left(\frac{2\pi}{\gamma(\alpha)}\right) \tag{61}$$

Yet, the sum on the r.h.s. in Eq. (61) is on the index for which $Q_{jk} \in \Omega$. The link between variables (x,y) and (u,v) is given by

$$u = \frac{1}{\gamma}\left[\left(R' \cos\alpha - R \sin\alpha\right) x + \left(R \cos\alpha + R' \sin\alpha\right) y - RR'\right] \tag{62}$$

$$v = \frac{1}{\gamma}\left[-\left(R \cos\alpha + R' \sin\alpha\right) x + \left(R' \cos\alpha - R \sin\alpha\right) y + R^2\right] \tag{63}$$

with the inverses

$$x = \frac{1}{\gamma}\left[\left(R' \cos\alpha - R \sin\alpha\right) u - \left(R \cos\alpha + R' \sin\alpha\right) v\right] + R\cos(\alpha) \tag{64}$$

$$y = \frac{1}{\gamma}\left[\left(R \cos\alpha + R' \sin\alpha\right) u + \left(R' \cos\alpha - R \sin\alpha\right) v\right] + R\sin(\alpha) \tag{65}$$

In Eqs (62)–(65), γ, R and R' are computed at α. By putting

$$w = u + iv, z = x + iy, \lambda = \frac{1}{\gamma}\left(R + iR'\right) \tag{66}$$

We may write Eqs (62)–(65) in the very synthetic form

$$w = i\lambda\left(R - e^{-i\alpha} z\right) \tag{67}$$

$$z = e^{i\alpha}\left(i\bar{\lambda} w + R\right) \tag{68}$$

By taking the Fourier expansion of $R(\vartheta)$, that is

$$R(\vartheta) = \sum_0^{\infty} \left(A_r \cos(r\vartheta) + B_r \sin(r\vartheta)\right) \tag{69}$$

The condition $(x,y) \in \Omega$ becomes

$$|z| < A_0 + \sum_1^{\infty} \frac{1}{|z|^n}\left(A_n \operatorname{Re}(z^n) + B_n \operatorname{Im}(z^n)\right) \tag{70}$$

In conclusion, by setting

$$w_{jk} = R\delta e^{ij\delta} \tag{71}$$

$$z_{jk} = e^{i\alpha}\left(i\bar{\lambda} w_{jk} + R\right) \tag{72}$$

From (70) to (72), the condition $Q_{jk} \in \Omega$ can be written as follows

$$|z| < A_0 + \sum_{1}^{\infty} \frac{1}{|z_{jk}|^{n}} \left(A_n \ \mathrm{Re}\left(z_{jk}^{n}\right) + B_n \ \mathrm{Im}\left(z_{jk}^{n}\right)\right) \quad (73)$$

For example, when $R(\vartheta) = \frac{1}{1+a}(1 + a \cos\vartheta), 0 \le a \le 1/2$ (lima on de Paschal), inequality (73) becomes

$$(1+a)|z_{jk}|^2 - |z_{jk}| - a x_{jk} < 0 \quad (74)$$

where $x_{jk} = \mathrm{Re}\, z_{jk}$.

In the case of the curvan crack, that is in dimensionless form

$$R(\vartheta) = (1 + a \cos 4\vartheta) \quad (75)$$

with a real number, the normalisation in such a way that $\max_{[0,2\pi]} \gamma = 1$ gives the equation of the contour

$$R(\vartheta) = \lambda'(1 + a \cos 4\vartheta) \quad (76)$$

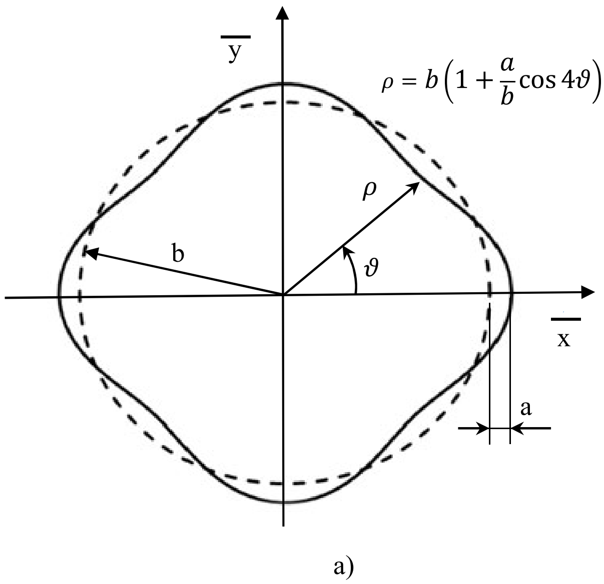

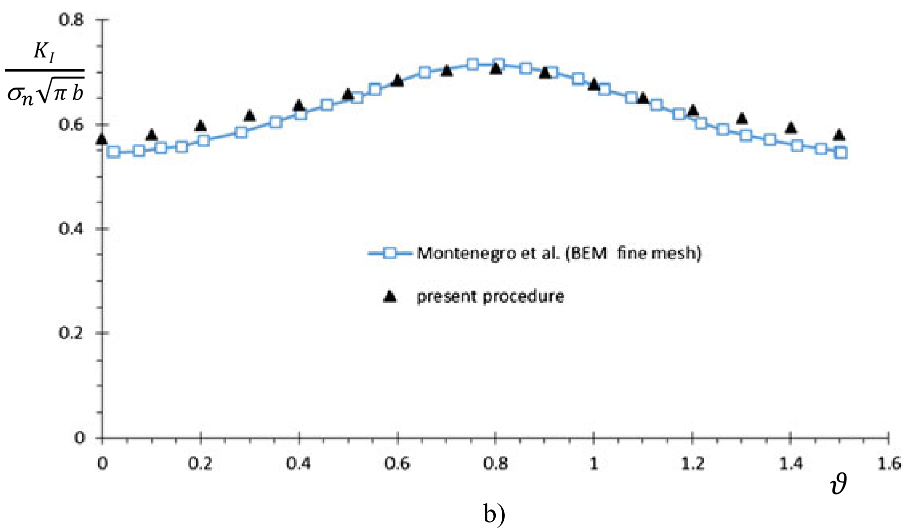

Fig. 9 (a) Curvan crack subjected to remote uniform tensile stress σ; (b) stress intensity factor in dimensionless form $\frac{K_I}{\sigma_n\sqrt{\pi b}}$ (σ_n nominal tensile stress, a/b = 0.1; M = 200). [Colour figure can be viewed at wileyonlinelibrary.com]

where λ' is defined as

$$\lambda' = \begin{cases} \dfrac{1}{1+a}; & 0 \le a \le \dfrac{1}{15} \\ \dfrac{\sqrt{15}}{4\sqrt{1+15a^2}}; & a \ge \dfrac{1}{15} \end{cases} \quad (77)$$

In general, this operation could be made numerically by imposing a rescaling of the dimensionless contour with a λ' scale factor. The SIF of the star domain will be that calculated by means of Eq. (60) dividing by $\sqrt{\lambda'}$.

The condition $Q_{jk} \in \Omega$ is

$$|z_{jk}|^5 - p|z_{jk}|^4 - pa\left(x_{jk}^4 - 6x_{jk}^2 y_{jk}^2 + y_{jk}^4\right) < 0 \quad (78)$$

where $y_{jk} = \mathrm{Im}\, z_{jk}$.

Figures 9 and 10 show a comparison from the results given by Eq. (60) and the results present in the literature[25,31] for a curvan crack and a half-circle and half $\rho = f(\vartheta) = \frac{A}{\sqrt{1+\left(\frac{A^2}{a^2}-1\right)|\sin\vartheta|}}$ with $A/a = 1.5$. The agreement is around some units per cent.

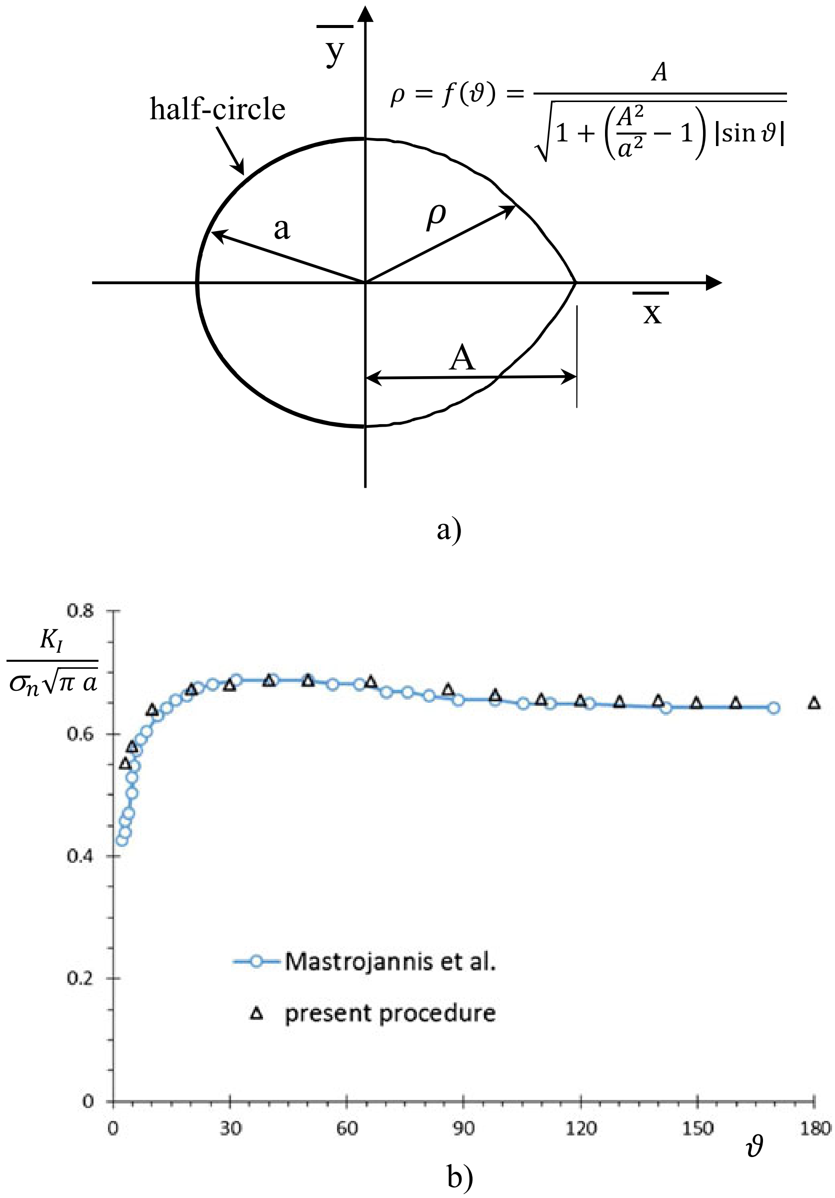

Fig. 10 (a) Half-circle and a shape whose polar equation is $\rho = f(\vartheta)$ subjected to remote uniform tensile stress σ, $A/a = 1.5$; (b) stress intensity factor in dimensionless form $\frac{K_I}{\sigma_n\sqrt{\pi a}}$ ($M = 200$). [Colour figure can be viewed at wileyonlinelibrary.com]

CONCLUSIONS

In this study, a very accurate procedure was proposed for the evaluation of the SIF by means of the Oore–Burns weight function. For defects similar to a star domain, an explicit algorithm was developed and the equations can be implemented in standard mathematical software. The high accuracy reached allows us to use a course mesh for the computation of the SIF of a crack with a general shape. A detailed analysis of the SIF at the tip of an elliptical crack shows that the OB integral gives maximum errors around 10% also for a small curvature radius.

REFERENCES

1 Glinka, G. and Shen, G. (1991) Universal features of weight functions for cracks in mode I. *Eng. Fract. Mech.*, **40**, 1135–1146.
2 Sha, G. T. and Yang, C. T. (1986) *Weight Function of Radial Cracks Emanating From a Circular Hole in a Plate*, ASTM: Philadelphia, pp. 573–600.
3 Zheng, X. J., Glinka, G. and Dubey, R. N. (1996) Stress intensity factors and weight functions for a corner crack in a finite thickness plate. *Eng. Fract. Mech.*, **54**, 49–61.
4 Fett, T. (2000) Failure due to semielliptical surface cracks under arbitrary stress distributions. *Fatig. Fract. Engng. Mater. Struct.*, **23**, 347–353.
5 Zheng, X. J., Glinka, G. and Dubey, R. N. (1995) Calculation of stress intensity factors for semielliptical cracks in a thick-wall cylinder. *Int. J. Pres. Ves. Pip.*, **62**, 249–258.
6 Salvati, E., Livieri, P. and Tovo, R. (2013) Fattori di intensificazione delle tensioni per cricche ad angolo triangolari in corrispondenza di intersezione di fori sollecitate a modo I. *Frattura ed Integrità Strutturale*, **26**, 80–91.
7 Murakami, Y. and Endo, M. (1983) Quantitative evaluation of fatigue strength of metals containing various small defects or cracks. *Eng. Fract. Mech.*, **17**, 1–15.
8 Murakami, Y. (2002) *Metal Fatigue: Effects of Small Defects and Nonmetallic Inclusions*, 1st ed, Elsevier Science Ltd: New York.
9 Murakami, Y. and Nemat-Nasser, S. (1983) Growth and stability of interacting surface flaws of arbitrary shape. *Eng. Fract. Mech.*, **17**, 193–210.
10 Krasowsky, A. J., Orynyak, I. V. and Gienko, A. Y. (1999) Approximate closed form weight function for an elliptical crack in an infinite body. *Int. J. Fract.*, **99**, 117–130.
11 Orynyak, I., Batura, A. and Oryniak, A. (2016) Comparison of two numerical procedures for solution of the integro-differential equation of flat crack problem. *Eng. Fract. Mech.*, **160**, 185–198.
12 Oore, M. and Burns, D. J. (1980) Estimation of stress intensity factors for embedded irregular cracks subjected to arbitrary normal stress fields. *J Press Vess-T ASME*, **102**, 202–211.
13 Al-Falou, A. A. and Ball, R. C. (2000) The 3-D weight functions for a quasi-static planar crack. *Int. J. Solids Struct.*, **37**, 5079–5096.
14 Saeidi Googarchin, H. and Ghajar, R. (2014) Stress intensity factors calculation for surface crack in cylinders under longitudinal gradient pressure using general point load weight function. *Fatigue Fract. Eng. Mater. Struct.*, **37**, 184–194.
15 Ghajar, R. and Alizadeh, K. J. (2013) Mixed mode stress intensity factors for elliptical subsurface cracks in an elastic half-space subjected to a uniform normal loading. *Fatigue Fract. Eng. Mater. Struct.*, **36**, 1199–1208.
16 Alizadeh, K. J. and Ghajar, R. (2015) Calculation of mixed mode stress intensity factors for an elliptical subsurface crack under arbitrary normal loading. *Fatig. Fract Engng Mater. Struct.*, **38**, 700–713.
17 Grueter, L., Huget, W. and Kylla, H. (1984) Weight functions and stress intensity magnification factors for elliptical and semi-elliptical cracks under variable normal stress—part I, Z. *Werkstoffrech*, **15**, 10–17.
18 Beghini, M., Bertini, L. and Gentili, A. (1997) An explicit weight function for semi-elliptical surface cracks. *J. Press Vess-T ASME*, **119**, 216–223.
19 He, Z., Kotousov, A. and Berto, F. (2015) Effect of vertex singularities on stress intensities near plate free surfaces Fatig. *Fract. Engng. Mater. Struct.*, **38**, 860–869.
20 Pook, L. P. (2013) A 50-year retrospective review of three-dimensional effects at cracks and sharp notches. Fatigue. *Fract. Engng. Mater. Struct.*, **36**, 699–723.
21 Campagnolo, A., Meneghetti, G. and Berto, F. (2016) Rapid finite element evaluation of the averaged strain energy density of mixed-mode (I + II) crack tip fields including the T-stress contribution. *Fatigue Fract. Engng. Mater. Struct.*, **39**, 982–998.
22 Lazzarin, P., Livieri, P., Berto, F. and Zappalorto, M. (2008) Local strain energy density and fatigue strength of welded joints under uniaxial and multiaxial loading. *Eng. Fract. Mech.*, **75**, 1875–1889.
23 Song, W., Liu, X., Berto, F., Wang, P. and Fang, H. (2017) Fatigue failure transition analysis in load-carrying cruciform welded joints based on strain energy density approach. *Fatigue Fract. Engng. Mater. Struct.*, **40**, 1164–1177.
24 Desjardins, J. L., Burns, D. J. and Thompson, J. C. (1991) A weight function technique for estimating stress intensity factors for cracks in high pressure. *J Press Vess-T ASME*, **113**, 10–21.
25 Montenegro, H. L., Cisilino, A. P. and Otegui, J. L. (2008) A weight function method for the assessment of partially closed three-dimensional plane cracks. *Eng. Fract. Mech.*, **75**, 4486–4500.
26 Livieri, P. and Segala, F. (2015) New weight functions and second order approximation of the Oore–Burns integral for elliptical cracks subject to arbitrary normal stress field. *Eng. Fract. Mech.*, **138**, 100–117.
27 Livieri, P. and Segala, F. (2014) Sharp evaluation of the Oore–Burns integral for cracks subjected to arbitrary normal stress field. *Fatig. Fract Engng Mater Struct*, **37**, 95–106.
28 Irwin, G. R. (1962) Crack-extension force for a part-through crack in a plate. *J. Appl. Mech-T ASME*, **29**, 651–654.
29 Ascenzi, O., Pareschi, L. and Segala, F. (2002) A precise computation of stress intensity factor on the front of a convex planar crack. *Int. J. Numer. Methods Eng.*, **54**, 241–261.
30 Livieri, P., Segala, F. and Ascenzi, O. (2005) Analytic evaluation of the difference between Oore–Burns and Irwin stress intensity factor for elliptical cracks. *Acta Mech.*, **176**, 95–105.
31 Mastrojannis, E. N., Keer, L. M. and Mura, T. (1979) Stress intensity factor for a plane crack under normal pressure. *Int. J Fract.*, **15**, 247–258.

APPENDIX

We denote by f_p the Riemann approximation of f, by choosing the projection of Q on $\partial\Omega$ as a starting point. Then, by Eq. (13) of a previous paper,[26] it follows

$$k_I \approx \frac{\sqrt{2}}{\pi}\ \delta \sum_{jk} \frac{h_P\left(Q_{jk}\right)}{k} + C\sqrt{\delta} \tag{A1}$$

where

$$h_p \approx \frac{1}{f_P} \tag{A2}$$

Now, let f_F be the Riemann approximation of f, by choosing the 'pole' Q' as the starting point. By replacing h_F with h_P in Eq. (A1), we introduce a correction given by

$$\text{correction} \approx -\frac{\sqrt{2}}{\pi}\ \sum \frac{1}{k}\left(h_F - h_P\right) Q_{jk} \tag{A3}$$

where

$$h_F \approx \frac{1}{f_F} \tag{A4}$$

Our problem is therefore a very precise evaluation of the function $h_f - h_b$. We need a picture in order to illustrate the situation (Fig. A1), where

$$f_P = \sum_{-M}^{M} \frac{\delta}{y^2 + m^2\delta^2} \tag{A5}$$

$$f_F = \sum_{-M}^{M} \frac{\delta}{y^2 + (m+\mu)^2\delta^2} \tag{A6}$$

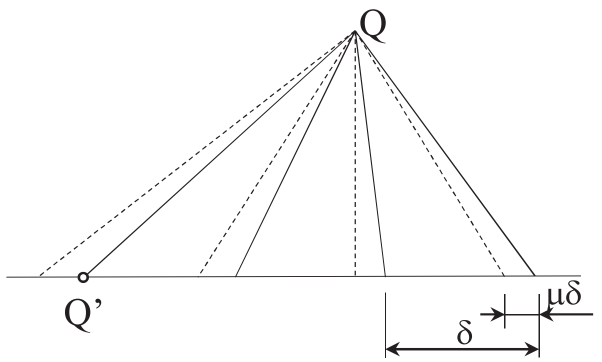

Fig. A1 Starting point from the pole Q'.

where $0 \le \mu \le \frac{1}{2}$ and $M\delta = 1$. By putting $a = \frac{y}{\delta}$, we may write

$$f_P = \frac{1}{\delta}\sum_{-M}^{M} \frac{1}{a^2 + m^2} \tag{A7}$$

$$f_F = \frac{1}{\delta}\sum_{-M}^{M} \frac{1}{a^2 + (m+\mu)^2} \tag{A8}$$

We consider three sets

$$X = \{(x,y),\ a \ge 1\} \tag{A9}$$

$$Y = \{(x,y), 0 \le a \le 1, |x| \ge \delta\} \tag{A10}$$

$$Z = \{(x,y), 0 \le a \le 1, |x| \le \delta\} \tag{A11}$$

The sets X,Y,Z are illustrated in Fig. A2. We begin by computing the contribution to the sum on the r.h.s. in Eq. (A3) coming from the region X. By the equation

$$\sum_{-\infty}^{+\infty} \frac{1}{a^2 + (m+\mu)^2} = \frac{\pi}{a}\ \frac{sh(2\pi a)}{ch(2\pi a) - \cos(2\pi\mu)} \tag{A12}$$

and Eq. (16), it follows that on the set X

$$f_F \approx f_P - \frac{R}{\delta} \tag{A13}$$

where

$$R = 2\left(\frac{\mu^2}{M^3} + \frac{\pi}{a}\ \frac{1 - \cos(2\pi\mu)}{e^{2\pi a}}\right) \tag{A14}$$

then

$$f_F \approx f_P + \frac{y^{3/4}R}{2\pi^{3/2}}\sqrt{\delta} \tag{A15}$$

This means that the conservation coming from the region X is about

$$-\frac{4\sqrt{2}\sqrt{\delta}}{\pi^{3/2}}\sum \frac{1}{\sqrt{k}}\ \sqrt{jk}\, e^{-2k\,\pi j\,\delta}\delta \approx$$
$$-\frac{4\sqrt{2}\sqrt{\delta}}{\pi^{3/2}}\sum \frac{1}{\sqrt{k}}\int_{1/k}^{1} \sqrt{t}\, e^{-2k\pi t} dt \approx\approx$$
$$-\frac{4\sqrt{2}\sqrt{\delta}}{\pi^{3/2}}\sum_{2}^{\infty} \frac{1}{k^2}\int_{1}^{\infty} \sqrt{u}\, e^{-2\pi u} du \approx 0.00020\sqrt{\delta} \tag{A16}$$

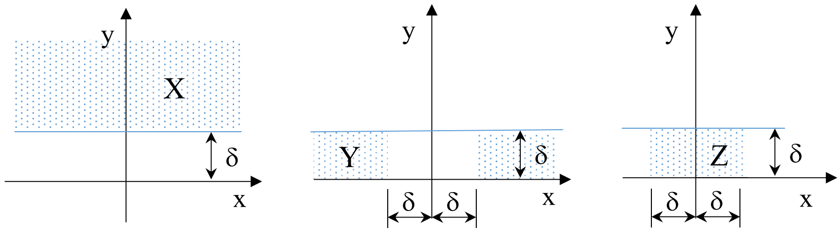

Fig. A2 Sets for the evaluation of correction C'. [Colour figure can be viewed at wileyonlinelibrary.com]

Now, we consider the contribution to the correction, due to the set Y. From Eq. (A12), it follows for small μ/a

$$f_F \approx \frac{1}{\delta} g_P - \frac{1}{\delta} S \mu^2 \tag{A17}$$

where

$$S = \frac{\pi^3}{a} \frac{1}{th(\pi a)} \frac{1}{sh^2(\pi a)} \tag{A18}$$

$$g_p = \frac{\pi}{a} \frac{1}{th(\pi a)} \tag{A19}$$

$$h_F \approx h_P + \frac{S\mu^2}{2 g_P^{3/2}} \sqrt{\delta} \tag{A20}$$

We take into account that in the region Y, $\mu \approx \frac{1}{2} k \vartheta^2$, where $\tan \vartheta = \frac{y}{x}$. Hence, the contribution is of the type

$$\begin{aligned}
&-\frac{\sqrt{2}\sqrt{\delta}}{4\pi} \sum k \frac{\delta(kj\delta)}{g_P^{3/2}(kj\delta)} \left(j^4 \delta^4\right) \delta \approx \\
&-\frac{\sqrt{2}\sqrt{\delta}}{4\pi} \sum k \int_0^{1/k} \frac{S(kt)}{g_P^{3/2}(kt)} t^4 \, dt \approx \\
&-\frac{\sqrt{2\pi}\sqrt{\delta}}{4} \sum_2^{\infty} \frac{1}{k^4} \int_0^1 \frac{u^{9/2}\sqrt{th(\pi u)}}{sh^2(\pi u)} du \approx \\
&-0.00031\sqrt{\delta}
\end{aligned} \tag{A21}$$

Hence, the only 'significant' contribution comes from the set Z. We divide Z in three subregions Z_1, Z_2, Z_3 (Fig. A3)

$$Z_1 = \left\{ (x, y) \in Z,\ 0 \le \sin \frac{y}{x} \le \frac{1}{2} \right\} \tag{A22}$$

$$Z_2 = \left\{ (x, y) \in Z,\ \frac{1}{2} \le \sin \frac{y}{x} \le \frac{\sqrt{3}}{2} \right\} \tag{A23}$$

$$Z = \left\{ (x, y) \in Z,\ \frac{\sqrt{3}}{2} \le \sin \frac{y}{x} \le 1 \right\} \tag{A24}$$

On the region Z_1, f_P is given by Eq. (A5), while

$$f_F = \sum \frac{\delta}{y^2 + (m\delta + x)^2} \tag{A25}$$

with $x \approx \delta\left(1 - \frac{\vartheta^2}{2}\right)$, $y \approx \delta\,\vartheta$, $\tan \vartheta = \frac{y}{x}$. We may write

$$f_P \approx \frac{1}{\delta}\left(\frac{1}{\vartheta^2} + \sum_{m \neq 0} \frac{1}{\vartheta^2 + m^2}\right) \approx \frac{1}{\delta\,\vartheta^2}\left(1 + \frac{\pi^2}{3}\vartheta^2\right) \tag{A26}$$

$$\begin{aligned}
f_F &\approx \frac{1}{\delta}\left(\frac{1}{\vartheta^2 + \frac{\vartheta^4}{4}} + \sum_{m \neq 0} \frac{1}{\left(\vartheta^2 + m + \frac{\vartheta^2}{2}\right)^2}\right) \\
&\approx \frac{1}{\delta\,\vartheta^2}\left(1 + \left(\frac{\pi^2}{3} - \frac{1}{4}\right)\vartheta^2\right)
\end{aligned} \tag{A27}$$

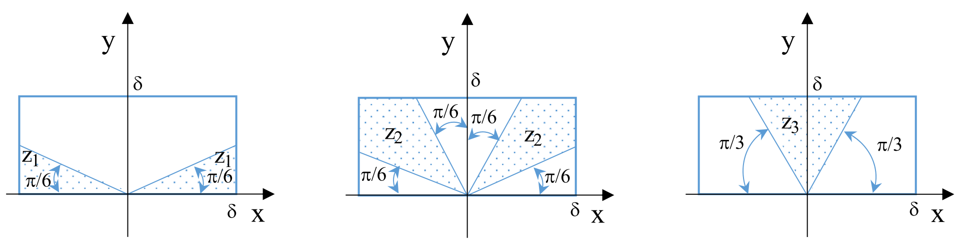

Fig. A3 Subsets of set Z. [Colour figure can be viewed at wileyonlinelibrary.com]

From Eqs (A26) and (A27), it follows

$$h_F - h_P \approx \frac{\sqrt{\delta}}{8} \frac{\vartheta^3}{\left(1+\pi^2 \frac{\vartheta^2}{3}\right)^{3/2}} \tag{A28}$$

By taking into account that on Z, k is fixed and equal to 1, the contribution is then given by

$$-\frac{\sqrt{2}\sqrt{\delta}}{4\pi} \int_0^{1/2} \frac{\vartheta^3}{\left(1+\pi^2 \frac{\vartheta^2}{3}\right)^{3/2}} d\vartheta \approx -0.00094\sqrt{\delta} \tag{A29}$$

In the region Z_3, in virtue of Eq. (A12), by putting $\tan\vartheta = \frac{y}{x}$, we make of the approximation

$$f_F \approx f_P - \frac{\pi^3 \, ch\,\pi}{sh^3\,\pi} \frac{\vartheta^2}{\delta} \approx f_P \left(1 - \frac{\pi^2}{sh^2\,\pi} \vartheta^2\right) \tag{A30}$$

The consequence of Eq. (A30) is

$$h_F \approx h_P + \frac{\pi^{3/2}\sqrt{th\,\pi}}{2\,sh^2\,\pi} \sqrt{\delta}\,\vartheta^2 \tag{A31}$$

The correction due to the set Z_3 is then given by

$$-\frac{\sqrt{2\pi}\sqrt{th\,\pi}}{sh^2\,\pi} \sqrt{\delta} \sum (j\delta)^2 \delta \approx -\frac{\sqrt{2}\,\pi^{7/2}\sqrt{th\,\pi}}{648\,sh^2\,\pi} \sqrt{\delta} \approx -0.00090\sqrt{\delta} \tag{A32}$$

Table A1 Calculation for region Z_2 (Fig. A3)

x/δ	y^2/δ	$(h_F - h_P)/\sqrt{\delta}$
0.500	0.750000	0.0045
0.609	0.629119	0.0061
0.707	0.500151	0.0071
0.750	0.437500	0.0072
0.793	0.371151	0.0071
0.866	0.255044	0.0058

(note that on Z, k is fixed an equal to the unity). Finally, we conclude by computing the correction due to the region Z_2. Here, we make use of a numerical procedure. From the results reported in Table A1, it follows the contribution on Z_2:

$$-\frac{\sqrt{2}}{3}\, 0.00638\sqrt{\delta} \approx -0.00300\sqrt{\delta} \tag{A33}$$

Summing up Eqs (A16), (A21), (A29), (A31) and (A33), we obtain

$$\text{correction} \approx -5.35\cdot 10^{-3}\sqrt{\delta} \tag{A34}$$

From Eqs (15) and (A34), we deduce the coefficient C' by choosing Q' as a starting point on $\partial\Omega$:

$$C' = 0.9275\ldots \tag{A35}$$